Tanzania Journal of Science 46(3): 859-872, 2020
ISSN 0856-1761, e-ISSN 2507-7961

Coal Exploration using Electrical Resistivity Method in Some Parts of Benue Trough, Nigeria

Saminu Olatunji and Abdulgafar T. Jimoh*
Department of Geophysics, University of Ilorin, P.M.B. 1515 Ilorin, Nigeria
**Corresponding author, e-mail: jimohabdulgafartosin94@gmail.com*
Co-author (Olatunji) e-mail: sam61ng@gmail.com
Received 10 Aug 2020, Revised 7 Oct 2020, Accepted 16 Oct 2020, Published Oct 2020
https://dx.doi.org/10.4314/tjs.v46i3.25

Abstract

Geoelectrical resistivity sounding technique was used to delineate the occurrence and extents of coal seam. Fifteen points were sounded with Schlumberger configuration in the suspected coal deposit site bounded by longitudes 7.344° E and 7.366° E, and latitudes 7.318° N and 7.33° N. The vertical electrical sounding (VES) data were analyzed and the corresponding geo-electric parameters at various depths were modeled. The earth model within the study area was correlated with available lithology of a nearby mine site. The sounding signatures are KQHK and KHK curve types which revealed five to six distinct geo-electrical equivalent layers. The wet to dry sandy topsoil has resistivity range of 300–1000 Ωm and average thickness of 1.5 m. Next is a layer with higher resistivity range (1000–20000 Ωm). This layer, which extends to 14 m depth, is considered probably to be laterite, patched with sand in some places. Underlain this is a shale formation that laterally sandwiched the coal seam. The thickness and resistivity range of the coal seam is 1.5–3.4 m and 778–103000 Ωm, respectively, while the shale domain has resistivity range of 99–898 Ωm. Therefore, it could be concluded that the coal seam occurrence take shale as host rock in the area and the largest deposit appeared at the Eastern part of the area.

Keywords: Benue trough; Resistivity; Electrical sounding; Coal seam; Overburden

Introduction

In recent years, the mass production and consumption of coal resources in Nigeria has greatly increased the economic and the social well-being. Coal, which is assumed to be formed from the accumulation and preservation of plant remains buried millions of years ago, refers to an organic sedimentary rock. Coal is the world most plentiful and extensively distributed fossil fuel with estimated reserves of approximately 1.1 trillion tonnes, ought to be sufficient for 150 years at present utilization (BPC 2019). In global electricity production, about 40% of coal fuel is required, and are likely to remain a key constituent of the fuel merge for power generation, with rising demands in developing countries (World Energy Council, 2016). According to a report from the investigation carried out by Sada (2012), Nigeria has estimated coal reserves of over 2.7 billion tonnes. Despite the reported occurrence of these amounts of deposits, Nigerian Government has paid just little attention to coal mining. Nowadays, geophysical methods find values in explorations owing to the high costs of core drilling method in the area of coal mine business.

Geo-electrical resistivity method plays a vital role in solid mineral exploration (Telford et al. 1990) particularly in the delineation of coal seam in complex geological environments, and has been adopted by several authors such as: Krishnamurthy (2009), Nthaba (2020). This is because it find its usefulness in mapping out vertical and the lateral extents of the coal seam with estimated overburden thickness. Thus, by combining data on the surface geological features with subsurface information obtained from geo-electrical investigations, one may define the subsurface features and details of the coal geometry.

Location

The surveyed area is part of the lower Benue Trough, between longitudes 7.344° E and 7.366° E, and latitudes 7.318° N and 7.33° N (Figure 1).

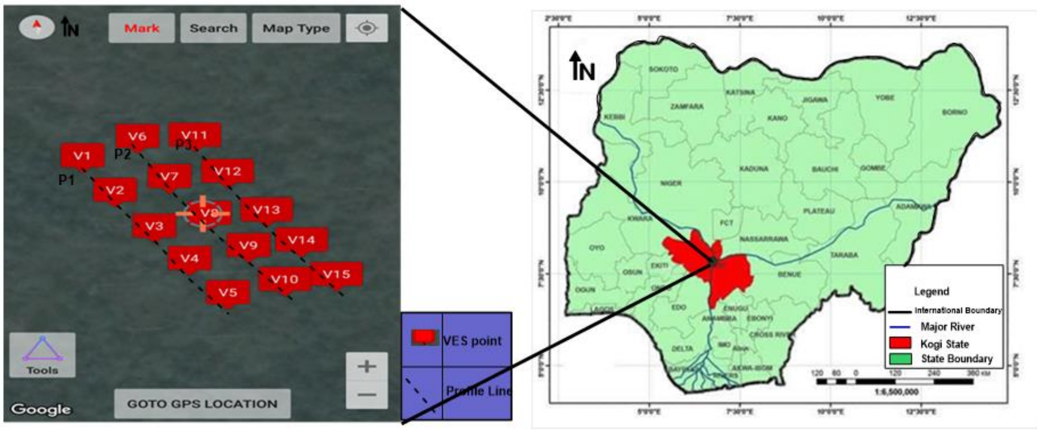

Figure 1: Study area map.

Geological highlight

The Lower Benue Trough lies in the southern part of the Trough (Figure 2). After the separation of the African plate and the South American plate, came the opening of the South Atlantic Oceans. Thus, the trough then originated as a consequence of failed arm of an aulacogen (Fatoye and Gideon 2013). Sedimentation in the Lower Benue Trough commenced with the marine Neocomian–Albian Asu River Group, although some pyroclastics of Aptian–Early Albian age have been scantly reported (Uzuakpunwa 1974, Ojoh 1992). Asu River Group was construed as sediments of the first transgressive cycle into the Lower Benue Trough. The Asu River Group sediments in the Lower Benue Trough comprises predominantly of shales with localized sandstones, siltstones and limestones (Olade 1975). It also consists of extrusive and intrusive material (Reyment 1965, Murat 1972, Nwachukwu 1972, Tijani et al. 1996) of the Abakaliki Formation in the Abakaliki area and the Mfamosing Limestone in the Calabar Flank (Petters 1982). Akande et al. (2011) confirmed that Asu River Group consists of arkosic sandstones, volcaniclastics, marine shales, siltstones and limestone which overly the Pre-Cambrian to Lower Paleozoic crystalline basement rocks. It was believed that the arkosic sediments were originated from the extensive weathering of the basement rocks, believed to be invaded by alkaline basaltic rocks prior to the initial rapid marine flooding of the Middle Albian times.

The marine Cenomanian–Turonian Nkalagu Formation (black shales, limestones and siltsones) and the interfingering regressive sandstones of the Agala and Agbani Formations (Cross River Group) rest on the Asu River Group. Although, sequences of sandstones, limestones and shales with calcareous sandstones of

Odukpani Formation were deposited unconformably on the Basement rocks in the Calabar Flank during the late Albian, the Santonian was a period of non-deposition, folding and faulting. This was followed by uplift and erosion of the sediments. The intensive Middle–Santonian deformation and magmatism in the Benue Trough displaced the major depositional axis westward which led to the formation of the Anambra Basin. Post deformational sedimentation in the Lower Benue Trough, therefore, constitutes the Anambra Basin.

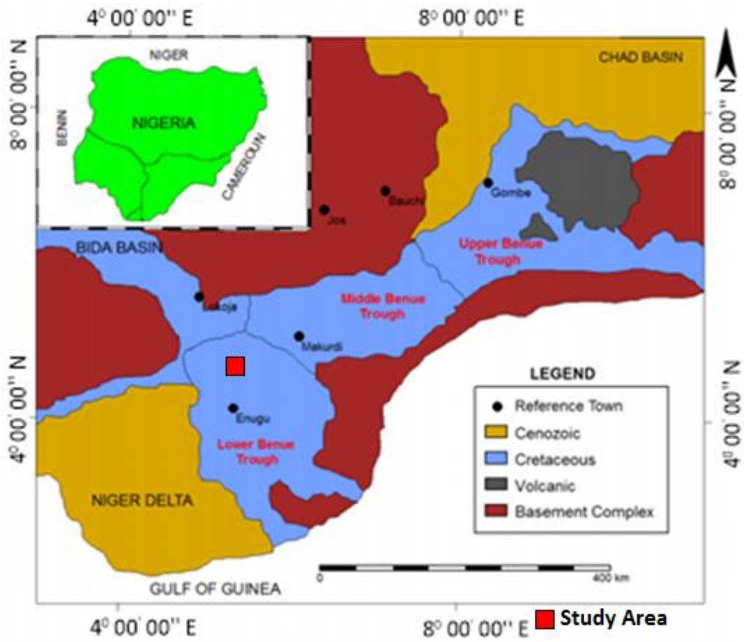

Figure 2: Simplified geology of Benue Trough (Obaje 1999).

Material and Methods

The recent study employed electrical resistivity method accomplished by applying VES technique which measures the variation of the electrical resistivity with depth. The changes in the electric resistivity values of geoelectrical section result from the material of the rock (density, shape, and porosity), water content, water quality and its content and temperature. So, the electric resistivity of porous formations has no limits (Parasnis 1962).

The Schlumberger array of electrode separation was used in this study by applying half spacing of current electrode (AB/2) starting from 1 to 100 m in successive steps. This involves spacing of four electrodes with two current electrodes widely spaced outside and two potential electrodes closely spaced within them along the survey profile (Figure 3).

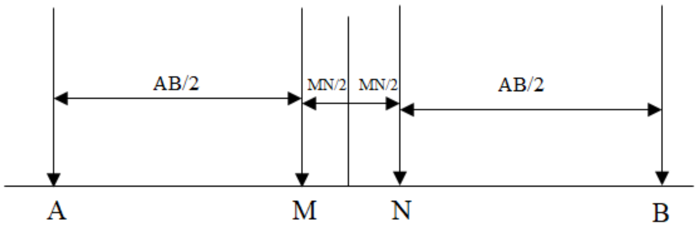

Figure 3: Schlumberger VES configuration (Kearey et al. 2002).

In this array, the potential electrodes MN can be fixed, while current electrodes A and B are changed. Telford (2004) recommended that MN < AB/5. The practical advantage of this is to minimize the effects of electrical noises. The aim of using this technique is to cover and reach the depth of the coal seam prone to the background information obtained from the study area. A total of 15 VES points, covering the suspected coal-deposit area along 3 profiles oriented Northwest-southeast direction were accomplished. This was carried out at 20 m inter-VES point and profile spacing, using *HEROJAT* resistivity meter (Figure 4). The resistivity meter used has been tested in theUniversity of Ilorin, Nigeria and results correlated well (90% correlation) with the results obtained with ABEM SAS 4000 Terrameter.

Figure 4: *Herojat* resistivity meter.

Based on the second Ohm's law: $\rho = \frac{AR}{L}$ (where ρ = resistivity, A = cross sectional area, L= length and R= resistance); so from Figure 3, apparent resistivity is derived as:

$$\rho_a = \frac{(^{AB}/_2)^2 - (^{MN}/_2)^2 \text{ x } \pi}{2(^{MN}/_2)} \text{ x } R \qquad (1)$$

and the geometric factor

$$G = \frac{(^{AB}/_2)^2 - (^{MN}/_2)^2 \text{ x } \pi}{2(^{MN}/_2)} \qquad (2)$$

Thus, $\rho_a = G \text{ x } R$ (3)

Practically, AB and MN at any instance is substituted in G expression and used in Equation 3 to obtain apparent resistivity as data set.

Using the previous geological information obtained from the nearby mine sites and the preliminary investigations carried out for lithological calibration, the qualitative and quantitative interpretations of the geo-electrical survey data along the various profiles were carried out. Several authors have adopted the quantitative interpretation of the geo-electrical resistivity measurements for different areas, among them are: Santos et al. (2006), El-Galladi et al. (2007), Sultan et al. (2004), Araffa (2009), Mohamaden (2005), Mohamaden and Shagar (2009), Abbas et al. (2008), Mohamaden (2009) and Bassey et al. (2019). The quantitative interpretations of the field data were done using generalized curve matching technique and *Ipi2win* (the inverse problem technique) software. Then results were represented as geoelectrical sections (Figures 8 to 10).

Further, the geo-electrical parameters obtained were then used to generate 2D and 3D maps using Surfer software package.

Results

Typical field curves generated from the interpretations of the VES data and layer parameters obtained in the area are shown in Figures 5 and 6. The geoelectric parameters are summarized in Table 1. For the purpose of lithological calibration from resistivity responses, a location where manual mining activity was going on showing the top of the coal seam was visited and a reference electrical sounding was done closer to the point (Figure 7).

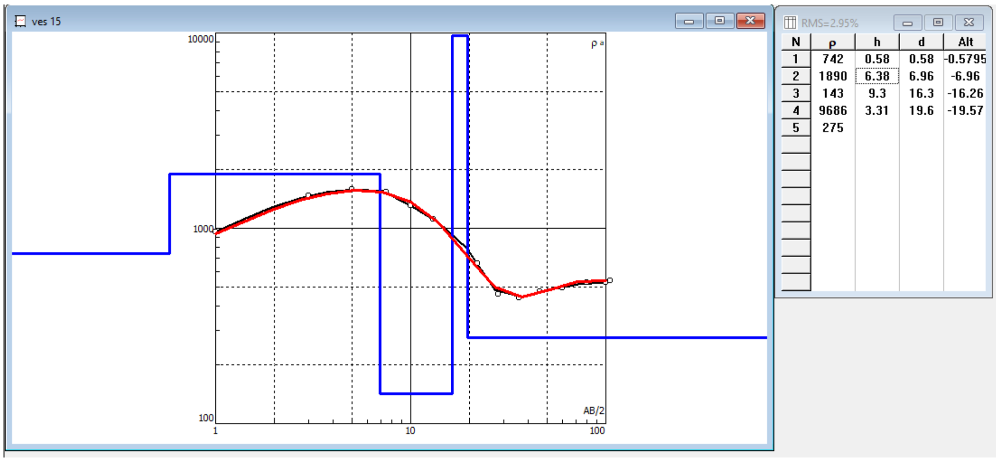

Figure 5: Typical field curve for VES 3.

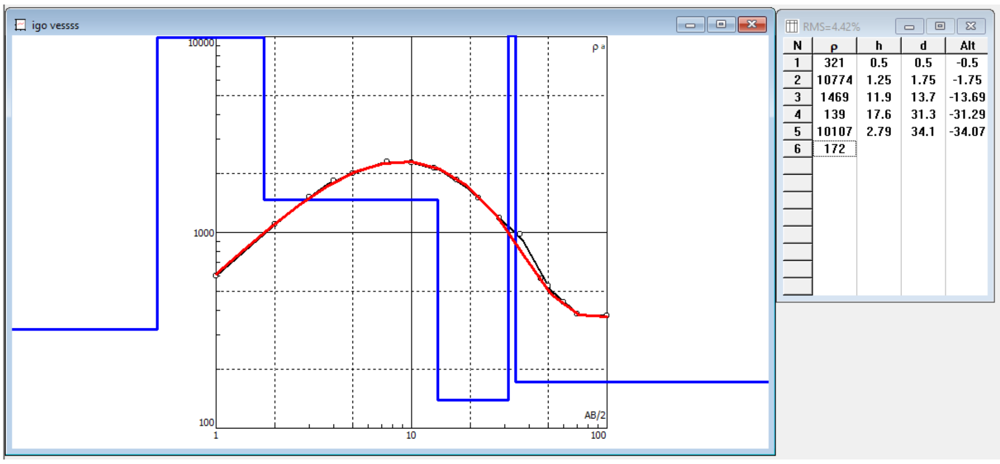

Figure 6: Typical field curve for VES 15.

Table 1: Geo-electric parameters summarized

VES station	No of layers	Resistivity (Ω-m)	Thickness (m)	Depth to layer end (m)	Curve type	Lithology
1	5	364	1	1	KHK	Topsoil
		15081	2.43	3.43		Laterite
		83.6	14.9	18.3		Shale
		39429	2.6	20.9		Coal
		1034	--	--		Shale
2	5	630	0.5	0.5	KHK	Topsoil
		3398	4.5	5		Laterite
		103	24.8	29.8		Shale
		10700	2	31.8		Coal
		167	--	--		Shale
3	6	321	0.5	0.5	KQHK	Topsoil
		10774	1.25	1.75		Laterite
		1469	11.9	13.65		Sand
		139	17.6	31.25		Shale
		10187	2.79	34.04		Coal
		172	--	--		Shale
4	5	1035	1.03	1.03	KHK	Topsoil
		13315	2.52	3.55		Laterite
		243	24.65	28.2		Shale
		778	1.7	29.9		Coal
		150	--	--		Shale
5	5	409	0.51	0.51	KHK	Topsoil
		1873	4.65	5.2		Laterite
		898	14.9	20.1		Shale
		18841	2.5	22.6		Coal
		778	--	--		Shale
6	6	547	0.51	0.51	KQHK	Topsoil
		7218	0.77	1.2		Laterite
		2540	13.2	14.5		Sand
		196	21.1	36.1		Shale
		66671	2.3	38.4		Coal
		156	--	--		Shale
7	5	499	0.76	0.76	KHK	Topsoil
		9453	2.59	3.35		Laterite
		320	26.65	30		Shale
		61814	1.5	31.5		Coal
		230	--	--		Shale
8	6	534	0.5	0.5	KQHK	Topsoil
		20772	3	0.53		Laterite
		1439	3.01	3.51		Sand
		260	20.12	26.63		Shale
		7098	2.8	29.41		Coal
		156	--	--		Shale
9	6	556	0.5	0.5	KQHK	Topsoil

VES station	No of layers	Resistivity (Ω-m)	Thickness (m)	Depth to layer end (m)	Curve type	Lithology
		18625	0.68	1.18		Laterite
		1697	12.7	13.9		Sand
		99	15.2	29.2		Shale
		15970	2.5	31.7		Coal
		134	--	--		Shale
10	5	320	1.31	1.31	KHK	Topsoil
		2354	4.99	6.31		Laterite
		102	13.3	19.6		Shale
		29764	3.1	22.7		Coal
		145	--	--		Shale
		957	1.05	1.05		Topsoil
11	6	22825	2.34	2.39	KQHK	Laterite
		21500	7.76	10.15		Sand
		514	19	29.15		Shale
		27032	3.1	33.25		Coal
		432	--	--		Shale
		878	0.74	0.74		Topsoil
12	5	5401	5.08	1.75	KHK	Laterite
		534	23.25	25		Shale
		7546	2.6	27.6		Coal
		621	--	--		Shale
		1035	1.03	1.03		Topsoil
13	5	13315	2.25	3.55	KHK	Laterite
		243	15.65	19.2		Shale
		778	3.4	22.6		Coal
		334	--	--		Shale
		832	0.74	0.74		Topsoil
14	5	11770	2.01	2.75	KHK	Laterite
		112	19.45	22.2		Shale
		103070	2.72	24.92		Coal
		323	--	--		Shale
		472	0.58	1.39		Topsoil
15	5	1890	6.38	7.35	KHK	Laterite
		143	9.3	19.6		Shale
		9686	3.31	19.6		Coal
		275	--	--		Shale

2D pseudo-sections were generated from the raw resistivity data as obtained. Thus, Figures 8 to10 are the 2D pseudo-sections inferred from the combination of VES data on each profile, for the 3 traverses. Finally, the identified anomaly parameters derived from field curves and pseudo-sections are summarized in Table 2. Therefore, the overburden thickness, depth to the coal-top surface and the coal thickness maps for the area are shown in Figures 11 to 13.

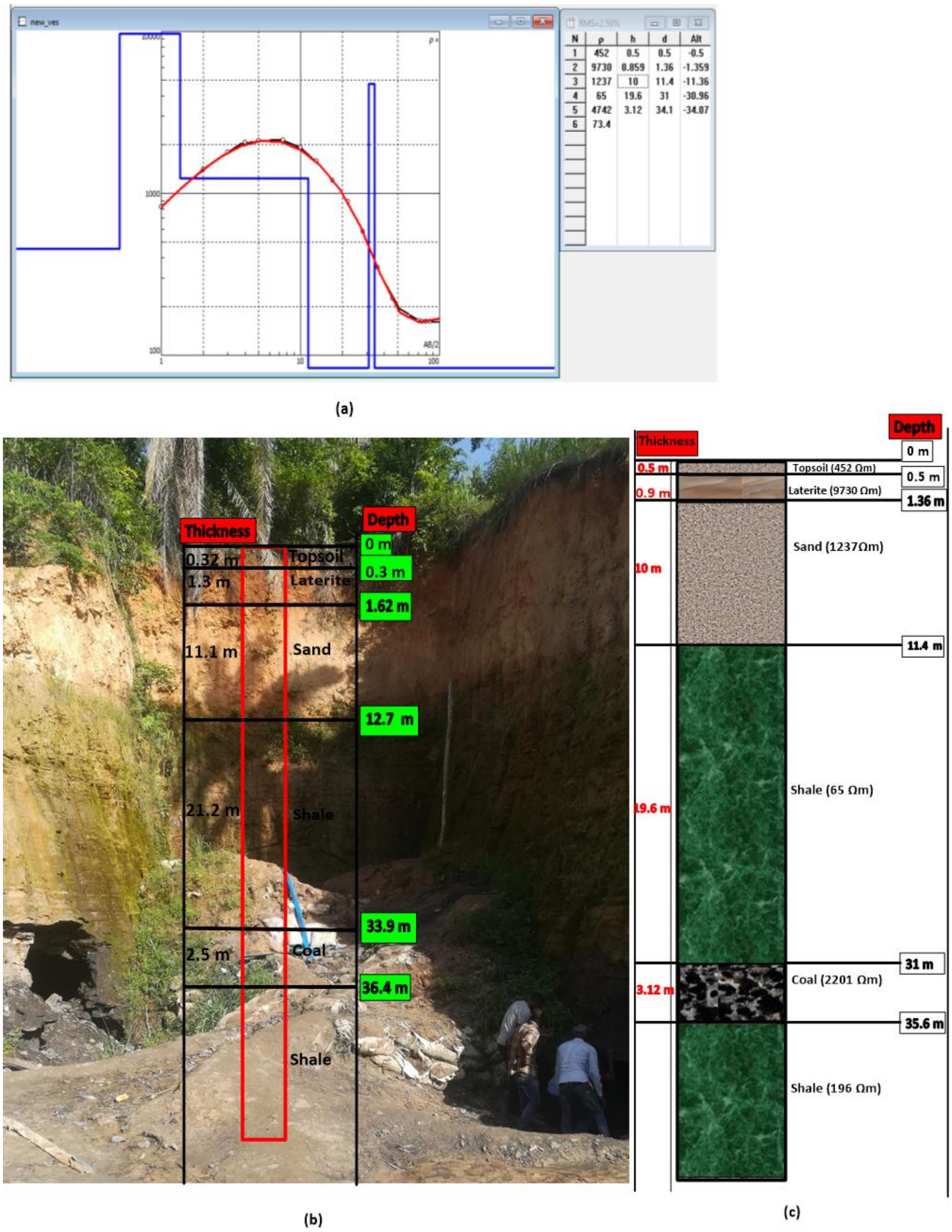

Figure 7: Correlation of lithological log with VES model at a mining site within the study area; (a) VES curve for the modeled site, (b) Observed lithology at the mining site, and (c) 1D geological equivalence of electrical response (used for lithological calibration).

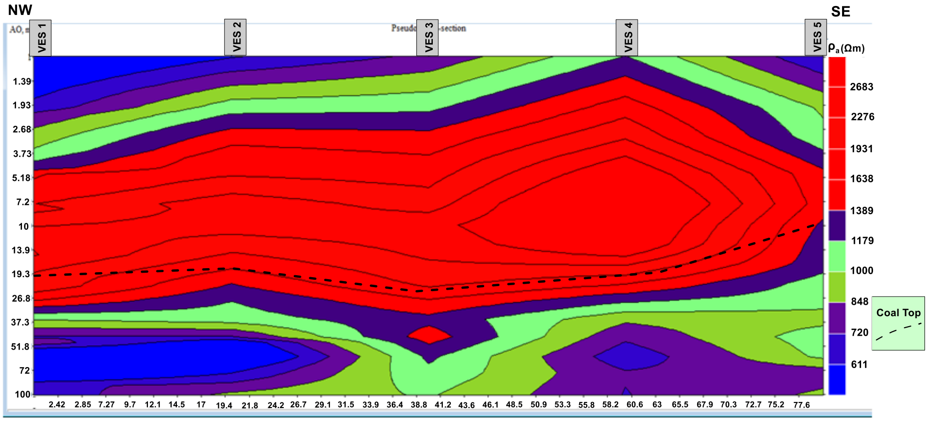

Figure 8: 2D pseudo-section along profile 1.

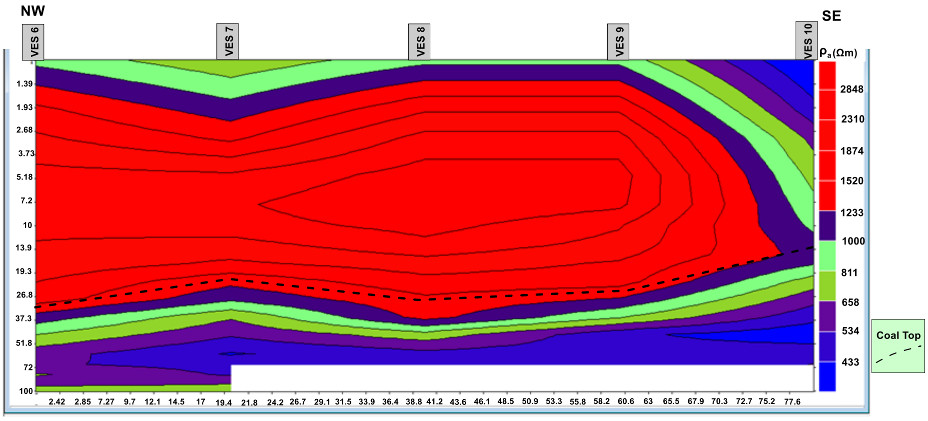

Figure 9: 2D pseudo-section along profile 2.

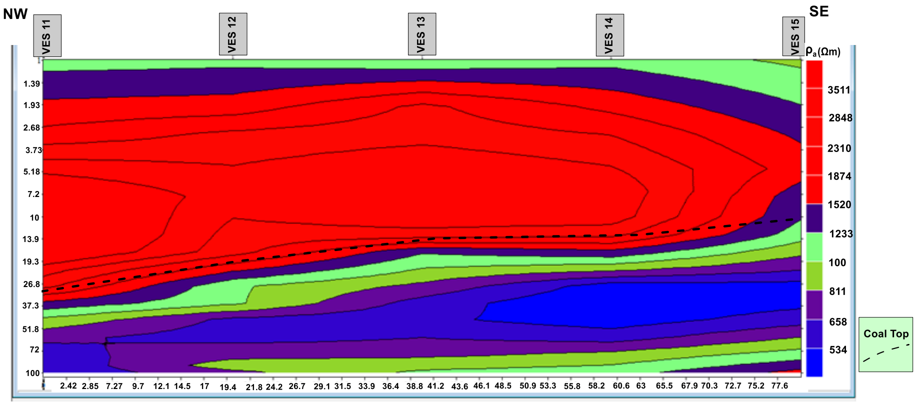

Figure 10: 2D pseudo-section along profile 3.

Table 2: Anomaly parameters

VES station	Overburden thickness (m)	Coal thickness (m)
1	18.3	2.6
2	29.8	2
3	31.3	3
4	28.2	1.7
5	20.1	2.5
6	36	2.3
7	30	1.5
8	26.3	2.8
9	29.1	2.5
10	19.6	3.1
11	30	3.1
12	25	2.6
13	19.2	3.4
14	22	2.7
15	19.6	3.2

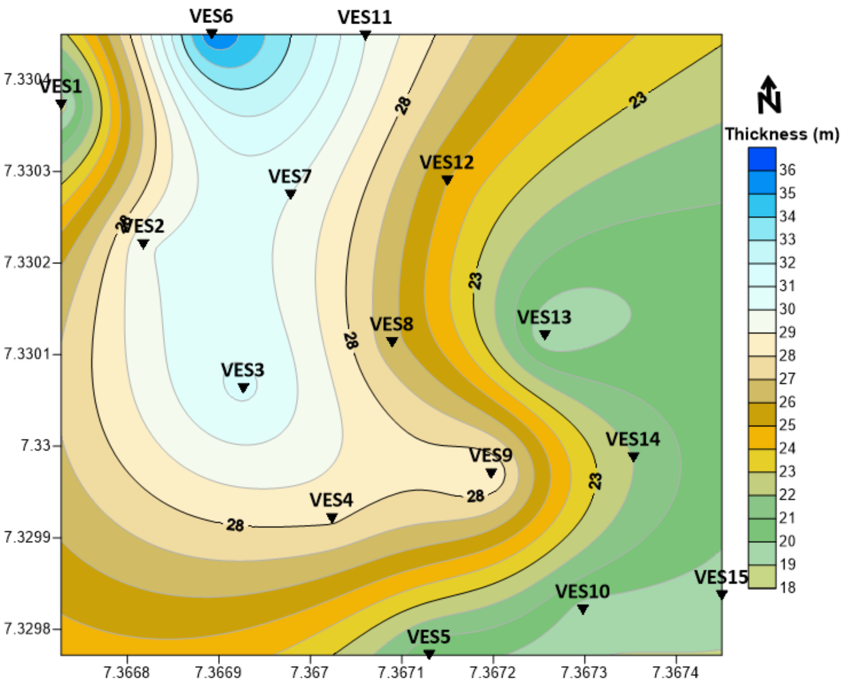

Figure 11: 2D Overburden thickness map.

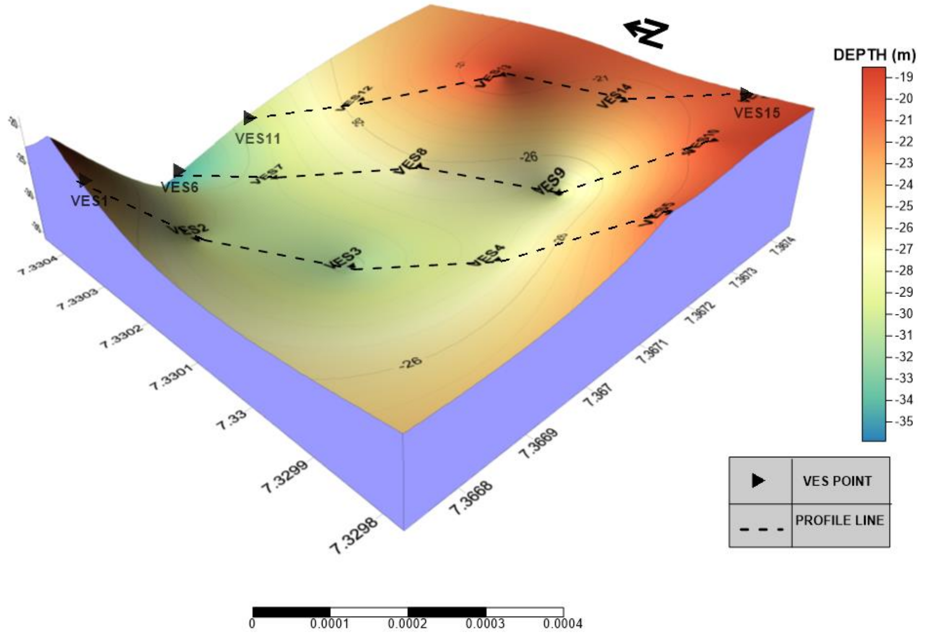

Figure 12: 3D Coal-top surface map.

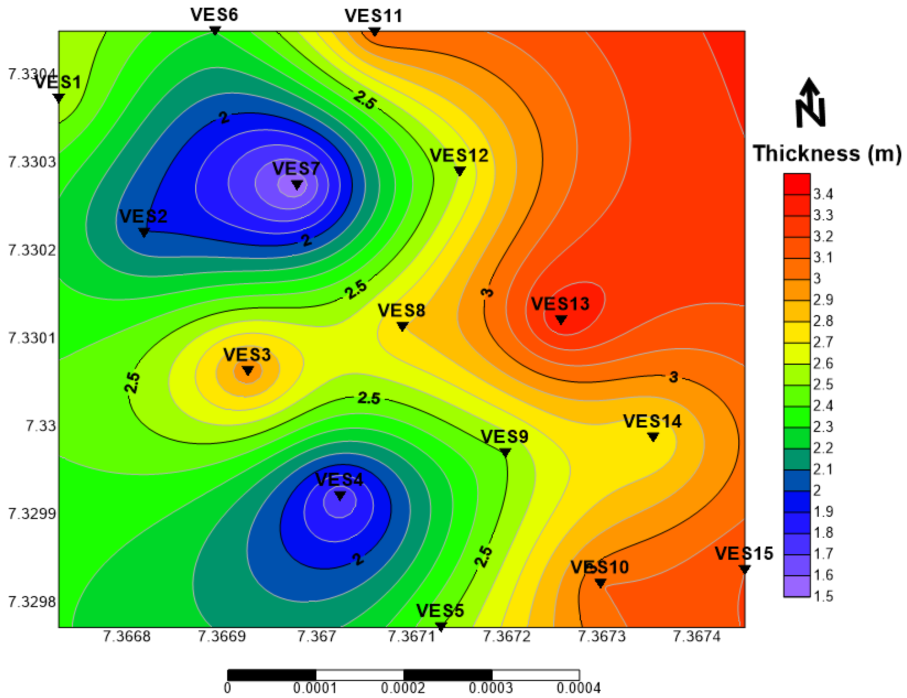

Figure 13: 2D Coal thickness map.

Discussion

The salient features of the subsurface parameters obtained from the fifteen vertical electrical soundings conducted in some part of Nigeria Lower Benue Through (Figure 2), interpreted using curve matching technique and Ipi2win software are given in Table 1. The geo-electric sounding curve signatures of the study area are KQHK and HKH (Figure 5 and 6). These reveal predominant five to six layers. The first Layer which is identified as the topsoil comprises dry sand and/or laterite, with average resistivity of 700 Ωm and thickness ranging from 0.5 to 1 m. The depth of the next layer considered to be laterite, patched with sand in some places is 14 m; with resistivity range of 1000– 20000 Ωm. Shale formations that host coal seam fall below this layer. The thickness and resistivity range of the coal seam are 1.5–3.4 m and 778–103000 Ωm, respectively, while the shale domain has resistivity range of 99–898 Ωm.

Figures 8 to 10 show the vertical view of the measured apparent resistivity pseudo-sections and the resistivity model for the three profiles, respectively. On interpreting the observed data from the mining site used for calibration (Figure 7), the reference resistivity at a given depth to coal seam were known. This served as benchmark for the interpretations of the data obtained from the survey area. Thus, the depth at the point of inflection on the field curve which correlated with reference resistivity of calibration marks new formation considered to be coal top. The reference value was then traced at all VES points along a profile to obtain depth to coal seam. These points, representing coal top, were connected using black dash lines (Figure 8 to 10).

Table 2 shows the estimated overburden and coal thickness derived from the field curves for the three parallel profiles. Because overburden refer to any materials that overlain the anomaly, therefore, the depth to anomaly of interest (coal) is directly equal to the overburden thickness. These data were then used to produce 2D and 3D maps (Figure 11 to 13).

Figure 11 shows varying overburden thickness ranging from 18 to 36 m across the three profiles. Areas with lower thickness are seen towards the south–eastern part which corresponded to VES 5, VES 10, VES 13, VES 14 and VES 15. Also, the central and southwestern parts (VES 4, VES 8, VES 9, and VES 10) show intermediate thickness, where northeastern and some eastern parts which corresponded to VES 2, VES 3, VES 6, VES 7 and VES 11 indicated higher overburden thickness. That is to say, where there are thicker, intermediate and thinner overburden, thickness corresponded to deeper, intermediate and shallower depth to coal seam, respectively (Figure 12). Furthermore, the coal thickness map of the study area (Figure 13) shows greater thickness from north to south towards the eastern part (along profile three), with intermediate thickness towards western and central parts and low thickness towards the north-western and the south-western parts which corresponded to profiles one and two (VES 1 to 10).

Conclusion

The occurrences of coal seam in part of Nigeria Lower Benue Trough have been evaluated using Schlumberger array of electrical resistivity technique. It could be concluded that the coal seam occurrence take shale as host rock in the area. Further, the eastern part of the study area which corresponds to profile three appears to be the most promising area for mining, owning to the thin nature of the overburden (average 23 m) and thick coal seam (3 m).

Acknowledgement

The authors express appreciations to the leadership of Onicha Igo town for the warm receptions and humility accorded to us during the fieldworks for data collection.

Funding
This research did not receive any specific grant from funding agencies in the public, commercial, or not-for-profit sectors.

Declaration of Interest: The authors hereby declare that there is no conflict of interest whatsoever on this research.

References

Abbas MA, Sultan SA and Santos FAM 2008 2-D and 3-D resistivity in the area of the Menkaure Pyramid Giza, Egypt. B*ull. Eng. Geol. Environ* 67: 411-414.

Akande SO, Ojo OJ, Adekeye OA, Egenhoff SO, Obaje NG and Erdtman BD 2011 Stratigraphic evolution and petroleum potential of Middle Cretaceous sediments in the Lower and Middle Benue Trough, Nigeria: insights from new source rock facies evaluation. *Petroleum Technology Development Journal* 1:1-34.

Araffa SAS 2009 Geophysical investigation for shallow subsurface geotechnical problems of Mokattam area, Cairo, Egypt. *Environ. Earth Sci.* 59(6): p.1195.

Bassey P, Lawrence OO and Ailego J 2019 Geo-electrical Resistivity evaluation of groundwater potential at University of Benin Ugbowo Campus, Benin-City, Edo State of Nigeria, using the Schlumberger array. *J. Appl. Sci. Environ. Manage.* 23(9): 1761-1770.

BPC (British Petroleum Commission) 2019 Statistical review of world energy 68th edition. (https://www.bp.com/content/dam/bp/businesssites/en/global/corporate/pdfs/energy-economics/statistical-review/bp-stats-review-2019-full-report.pdf)

El-Galladi A, El-Qady G, Metwaly M and Awad S 2007 Mapping peat layer using surface geoelectrical methods at Mansoura environs, Nile Delta, Egypt. *Mansoura J. Geol. Geophys.* 34(1): 59-78.

Fatoye FB and Gideon YB 2013 Geology and mineral resources of the Lower Benue Trough, Nigeria. *Adv. Appl. Sci. Res.* 4(6): 21-28.

Kearey P and Brooks M and Hill I 2002 An introduction to geophysical exploration. Blackwell Publishing.

Krishnamurthy NS, Rao VA, Kumar D, Singh KKK and Ahmed S 2009 Electrical resistivity imaging technique to delineate coal seam barrier thickness and demarcate water filled voids. *J. Geol. Soc. India* 73: 639–650

Mohamaden MI and Shagar SA 2009 Structural effect on the groundwater at the Arish City, North eastern part of Sinai Peninsula, Egypt. *Egypt. J. Aquat. Res* 35(2): 31–47.

Mohamaden MI 2009 Groundwater exploration at Rafah, Sinai Peninsula, Egypt. *Egyp. J. Aquat. Res.* 35(2): 49–68.

Mohamaden MI 2005 Electric resistivity investigation at Nuweiba harbour Gulf of Aqaba, South Sinai, Egypt. *Egypt. J. Aquat. Res.* 31(1): 58-67.

Murat C 1972 Stratigraphy and paleogeography of the Cretaceous and Lower Tertiary in South-Eastern Nigeria. In: Dessauvagie TFJ, Whiteman AJ (Eds), African Geology. *Ibadan University Press* 251-266.

Nthaba B, Shemang E, Hengari A, Kgosidintsi B and Tsuji T 2020 Characterizing coal seams hosted in Mmamabula Coalfield, central Botswana using pseudo-3D electrical resistivity imaging technique. *J. Afr. Earth Sci.* 103866.

Nwachukwu SO 1972 The tectonic evolution of the the southern portion of the Benue Trough, Nigeria. *Geological Magazine* 109: 411–419.

Obaje NG, Abaa SI, Najime T and Suh CE 1999 Economic geology of Nigerian coal resources-a brief review. *Afr. Geosci. Rev.* 6: 71-82.

Ojoh KA 1992 The southern part of the Benue Trough (Nigeria) Cretaceous stratigraphy, basin analysis, paleooceanography and geodynamic evolution in the Equatorial domain of the South Atlantic. *NAPE Bulletin* 7:67-74.

Olade MA 1975 Evolution of Nigerian’s Benue Trough (Aulacogen): a tectonic model. *Geol. Mag.* 112: 575-583.

Parasnis DS 1962 Principal of Applied Geophysics. Chapman and Hall limited. London 176 p.

Petters SW 1982 Central West African Cretaceous-Tertiary benthic foraminifera and stratigraphy. *Palaeontographica A* 179: 1-104.

Reyment RA 1965 Aspects of the Geology of Nigeria: the stratigraphy of the Cretaceous and Cenozoic deposits. Ibadan University Press 133 p.

Sada MM 2012 Investment opportunities in Nigeria minerals and metals sector, *Paper presented at Africa Down Under International Conference, Perth, Western Australia* 19 p.

Santos FAM, Sultan SA, Represas P and El-Sorady AL 2006 Joint inversion of gravity and geoelectrical data for groundwater and structural investigation: application to the northwestern part of Sinai, Egypt. *Geophys. J. Int.* 165: 705–718.

Sultan S, Helal A and Santos FAM 2004 Geoelectrical application for solving geotechnical problems at two localities in greater Cairo, Egypt. *NRIAG J. Geophys* 3(1): 51-64.

Telford WM, Geldart LP and Sheriff RE 1990 Applied Geophysics, Cambridge University press.

Telford WM, Geldart LP and Sheriff RE 2004 Applied Geophysics, 2nd edn. Cambridge University Press, Cambridge.

Tijani MN, Loehnert EP and Uma KO 1996 Origin of saline groundwaters in the Ogoja area, Lower Benue Trough, Nigeria. *J. Afr. Earth Sci.* 23(2): 237-252.

Uzuakpunwa ADB 1974 The Abakaliki pyroclastics, Eastern Nigeria: New age and tectonic implications. *Geol. Mag.* 111: 65-70.

World Energy Council 2016 World energy resources. (https://www.worldenergy.org/assets/images/imported/2016/10/World-Energy-Resources-Full-report-2016.10.03.pdf)